Journal of Geophysical Research: Oceans

Supporting Information for

Seasonal to intraseasonal variability of the surface mixed layer in the Gulf of Oman

Estel Font [1], Bastien Y. Queste[1], and Sebastiaan Swart[1,2]

[1] Department of Marine Sciences, University of Gothenburg, Gothenburg, Sweden, [2]Department of Oceanography, University of Cape Town, Rondebosch, South Africa

Contents of this file

Figure S1 to S3

Introduction

The supporting information contains three additional figures. We provide a supporting figure to validate the glider data management (Figure S1). Seaglider 579 was deployed in March 2015 until the end of May 2015 (91 days) during the spring intermonsoon and Seaglider 510 was deployed in mid-December 2015 and recovered at the end of March 2016 (108 days) during the winter NW monsoon. The data shows the bias between the up and downcast of the corrected glider data profiles for each season. There is an evident deviation during both seasons in the measurements at the first meters of the downcast profiles, more prominent during spring. The temperature bias is caused by the warming of the sensors during the communication phase at the surface between dives. Strong solar radiation warmed the glider and its sensors, causing an artificial rise in potential temperature. The bias in the downcast profiles produces fictitious results when observing lateral gradients, hence only climb profiles are used in this study. We provide a figure to show the little spatial variability of the atmospheric variables (ERA5 products) (Figure S2) and a figure to validate the election of the ERA5 reanalysis product over TropFlux (Figure S3).

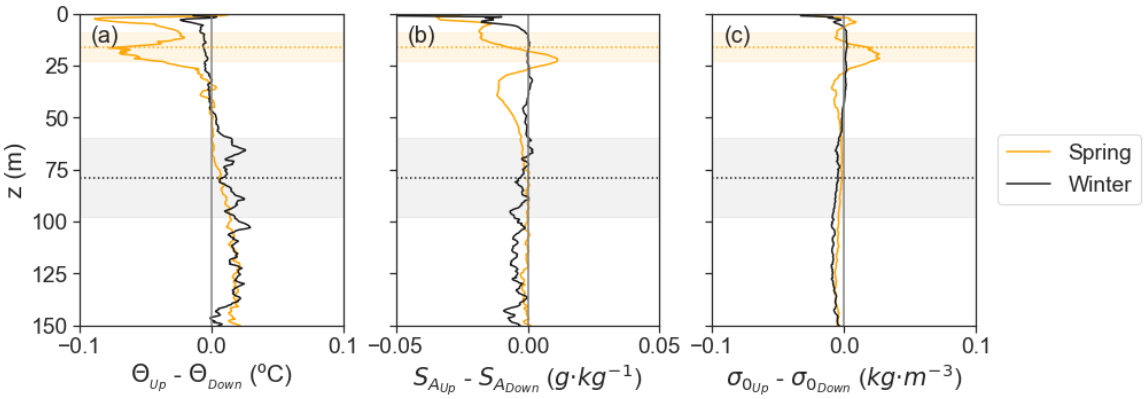

Figure S1. Temperature bias between up and downcast profiles. (a) Conservative temperature (Θ), (b) absolute salinity (S_A), and (c) potential density (σ_0) bias between up and downcast corrected data profiles for each season. The average MLD is displayed as the horizontal dotted line and the shading shows the STD. High air temperatures in the region cause warming of the sensors during the communication phase at the surface producing a bias in the measurements at the first meters of the downcast profiles. The deviation is evident during both seasons, although it is more prominent during spring when solar radiation is stronger.

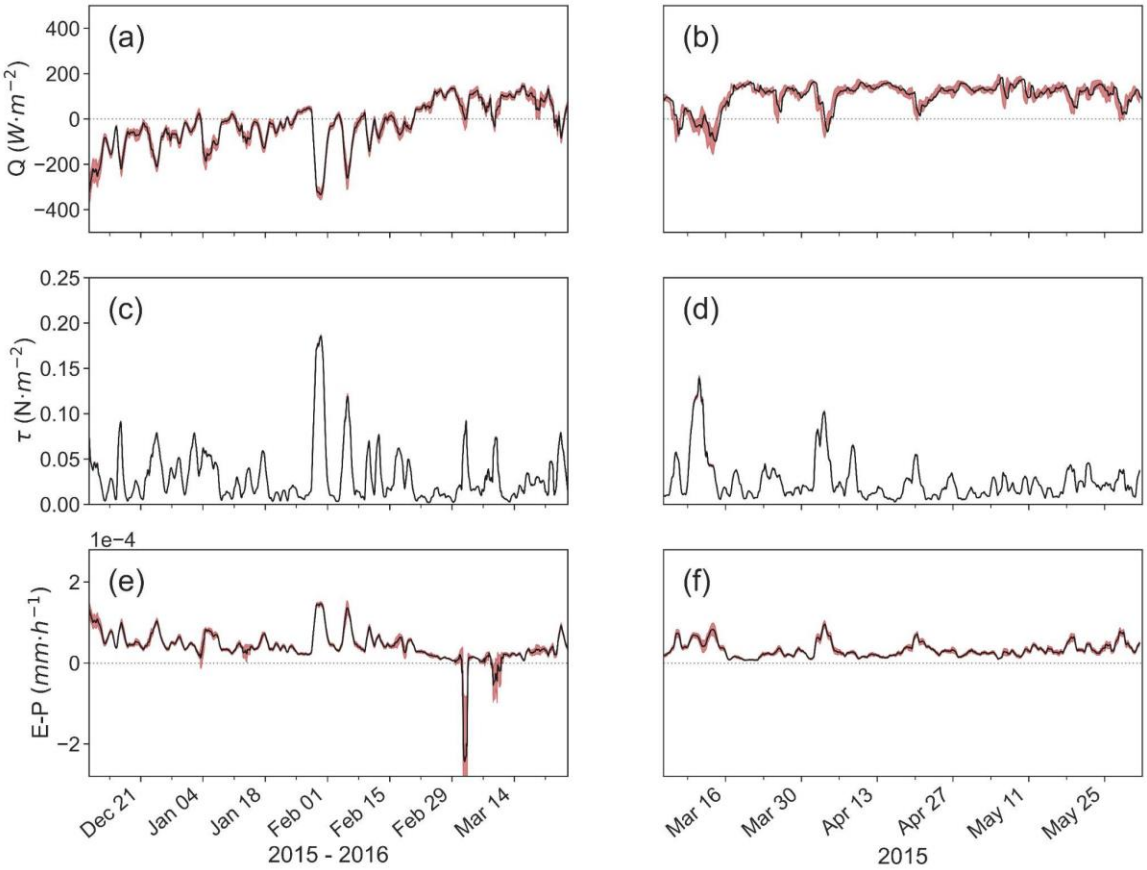

Figure S2. Spatial variability in the atmospheric forcing. Net heat flux (Q_{net}, black line), for winter (a) and spring (b). Wind stress (τ, black line) for winter (c) and spring (d). Freshwater flux, (E-P, black line) for winter (e) and spring (f). In red shading the standard deviation due to averaging the four ERA5 grid cells collocated on the glider transect. Notice that the standard deviation in the wind speed is very small and therefore not visible in panels c and d.

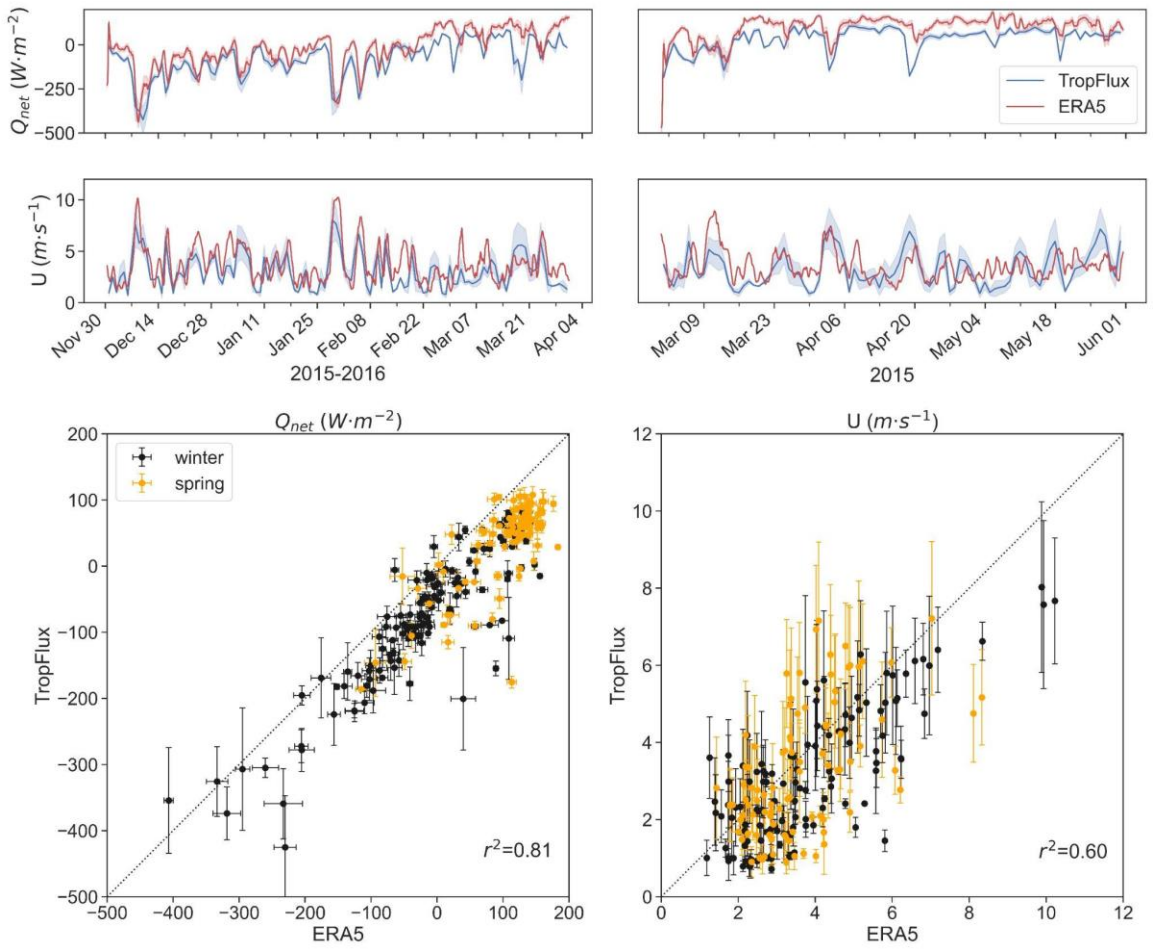

Figure S3. Comparison between ERA5 and Tropflux atmospheric forcing. ERA5 variables have been resampled to a daily resolution to compare to Tropflux products. Top panels compare the timeseries of net heat flux (Q_{net}) and wind speed (U) for ERA5 (red) and Tropflux (blue) for winter (fist column) and spring (second column). The shading shows the standard deviation. Daily mean biases between the products are (63 ± 48) $W \cdot m^{-2}$ in Q_{net} and (0.6 ± 1.3) $m \cdot s^{-1}$ in U. Bottom panels compare the ERA5 vs. Tropflux for Q_{net} (left) and U (right) for winter (black) and spring (orange). The error bars mark the standard deviation for each value. The dotted line shows the 1 to 1 relation between data sources. Correlation values (r^2) for all the data are displayed in the bottom panels.